



# Evaluating the Potential Benefits of Metal Ion Doping in SnO<sub>2</sub> Negative Electrodes for Lithium Ion Batteries<sup>☆</sup>



Mechthild Lübke<sup>a,b</sup>, Ding Ning<sup>b</sup>, Ceilidh F. Armer<sup>b,c</sup>, Dougal Howard<sup>a</sup>, Dan J.L. Brett<sup>d</sup>, Zhaolin Liu<sup>b</sup>, Jawwad A. Darr<sup>a,\*</sup>

<sup>a</sup> Department of Chemistry, University College London, 20 Gordon Street, London, WC1H 0AJ, UK

<sup>b</sup> Institute of Materials Research and Engineering (IMRE), A\*STAR (Agency for Science, Technology and Research), 2 Fusionopolis Way, Innovis #08-03, Singapore 138634, Republic of Singapore

<sup>c</sup> College of Engineering and Computer Science, Australian National University, Canberra, ACT 0200, Australia

<sup>d</sup> Electrochemical Innovation Lab, Department of Chemical Engineering, University College London, Torrington Place, London, WC1E 7JE, UK

## ARTICLE INFO

### Article history:

Received 13 March 2017

Received in revised form 4 May 2017

Accepted 6 May 2017

Available online 8 May 2017

### Keywords:

Continuous Hydrothermal Flow Synthesis

Tin dioxide

Lithium ion battery

Anode

Nano

## ABSTRACT

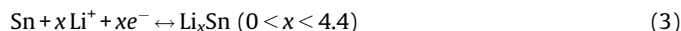
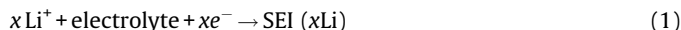
Nine different transition metal doped (<10 at%) tin dioxides and undoped SnO<sub>2</sub> nanopowders with similar specific surface areas were made using a continuous hydrothermal process and then investigated as potential negative electrode materials for lithium ion batteries. The as-prepared nanopowders were characterized via a range of analytical techniques including powder X-ray diffraction, X-ray photoelectron spectroscopy, X-ray fluorescence spectrometry, transmission electron microscopy, thermogravimetric analysis and Brunauer-Emmett-Teller surface area measurements. Doped SnO<sub>2</sub> materials were grouped into two classes according to the potential redox activity of the dopant (those presumed to be redox inactive: Nb, Ti, Zr; and those presumed to be redox active: Fe, Co, Cu, Zn, Mn, Ni). The role of the transition metal ion dopant on the cycling performance (overall capacity and voltage hysteresis), was elucidated for the first cycle via cyclic voltammetry measurements in half cells versus lithium metal. In particular, the authors were able to evaluate whether the initial Coulombic efficiency and the delithiation potential (vs. Li/Li<sup>+</sup>) of the doped samples, would be likely to offer any increased energy density (compared to undoped SnO<sub>2</sub>) for lithium ion batteries.

© 2017 The Author(s). Published by Elsevier Ltd. This is an open access article under the CC BY license (<http://creativecommons.org/licenses/by/4.0/>).

## 1. Introduction

High energy lithium ion batteries are a key technology with the potential to meet future requirements for energy storage in hybrid electric vehicles and other portable electronic devices [1,2]. High energy can be achieved with a high cell voltage (via a low operating voltage negative electrode and a high operating voltage positive electrode) and high specific capacities [3]. Conversion and alloying negative electrode materials have been shown to have very high theoretical capacities, e.g. Fe<sub>2</sub>O<sub>3</sub> = 1007 mAh g<sup>-1</sup>, Si = 3579 mAh g<sup>-1</sup>, Sn = 993 mAh g<sup>-1</sup>, and SnO<sub>2</sub> = 782 mAh g<sup>-1</sup> [1,4]. To date, alloying materials are favored compared to the conversion materials, due to the lower operating potential (vs. Li/Li<sup>+</sup>) and far lower voltage hysteresis of the former [4]. A voltage hysteresis can be understood

as a massive shift of the electrochemical potential activity from low potentials during lithiation, towards high potentials during delithiation for the negative electrode side. SnO<sub>2</sub> has attracted interest as a negative electrode in lithium ion batteries because it is relatively inexpensive, readily synthesized, non-toxic and shows high capacities [5–16]. The relevant electrochemical processes that occur during cycling are described in Equations 1–3:



Eq. (1) corresponds to the initial solid electrolyte interphase (SEI) formation during the first and following few cycles. The conversion of SnO<sub>2</sub> towards metallic Sn during initial lithiation, causes extreme structural and volume changes (Eq. (2)). During further lithiation, up to 4.4 mol of lithium ions are stored in

<sup>☆</sup> Research webpages <http://www.ucl.me.uk>.

\* Corresponding author at: Christopher Ingold Laboratories, Department of Chemistry, University College London, 20 Gordon Street, London, WC1H 0AJ, UK.  
E-mail address: [j.a.darr@ucl.ac.uk](mailto:j.a.darr@ucl.ac.uk) (J.A. Darr).

the metallic Sn at low potentials (Eq. (3)) and this reaction is considered fully reversible. There has been considerable disagreement regarding the reversibility of the conversion process shown in Equation 2; some researchers suggest this reaction is irreversible [17–19], whilst other researchers claim it is reversible [20–22]. The origin of this disagreement can be found in the additional delithiation capacity for high surface area SnO<sub>2</sub> materials at higher potentials (in the range ca. 1.2 to 2.0 V vs. Li/Li<sup>+</sup>). In an attempt to show the reversible formation of Sn<sup>4+</sup>, ex-situ X-ray photoelectron spectroscopy (XPS) measurements [21,23] and ex-situ high resolution-transmission electron microscopy (HR-TEM) studies [23,24] were used after the first delithiation step at ca. 3.0 V vs. Li/Li<sup>+</sup>. Conversely, Lee et al. suggested that the origin of this increased capacity could be mainly found in the electrochemical activity of LiOH/LiH/LiO<sub>2</sub> [25]; such species were also believed to be responsible for the additional storage capacities observed for RuO<sub>2</sub> (generated due to the presence of H<sub>2</sub>O, which leads to electrochemically active LiOH in the sample) [26]. Therefore, convincing evidence for a reversible conversion reaction is still missing to date, thus, we will not discuss this further herein.

Recently, several reports have claimed that the electrochemical performance of SnO<sub>2</sub> could be improved by introducing transition metal dopants into the host lattice or by addition of secondary metal oxide phases. Examples of such elements include Fe [5,27–29], Cu [30], Mn [29], Co [21,29,31,32], Co-Ni [12,33], Zn [34–36], Ti [37] and Ni [38,39]. More details can be found in a comprehensive review by Bresser et al. [40]. Unfortunately, only a few of the aforementioned studies reported the specific surface areas of the doped/composite SnO<sub>2</sub> and the pristine SnO<sub>2</sub> materials. Indeed, in some cases, the surface area of the pristine SnO<sub>2</sub> was more than three times lower than the corresponding doped SnO<sub>2</sub> [5,21]. In 2000, Li et al. highlighted the importance of using nano-sizing to improve the electrochemical properties of SnO<sub>2</sub> [41]. This was in agreement with others, who demonstrated drastic differences in the electrochemical performance with different particle sizes (essentially higher delithiation capacities with smaller particle sizes) [42,43]. Thus, in the evaluation of both pristine and doped SnO<sub>2</sub> materials, synthesis methods that can facilitate materials with both high and similar surface areas are highly desirable, because this may allow a better deconvolution of the effects of the dopants on the electrochemical properties (e.g. specific capacity and Coulombic efficiency).

Herein, the authors employed a continuous hydrothermal flow synthesis (CHFS) method to produce undoped and doped SnO<sub>2</sub> materials with similar (high) surface areas, crystallinity and dopant contents at a 10 g h<sup>-1</sup> production rate. The precursor concentrations used herein were with the dopant metal at a value of 10 at% (with respect to Sn). The CHFS process is described in more detail in the experimental section and supplementary information; the process has previously been used for the production of battery materials with high surface areas and narrow particle size distributions [44]. There are many negative electrode materials for lithium ion batteries that have been made via CHFS type processes, including anatase TiO<sub>2</sub> (undoped and doped with Sn or Nb) [45,46], Fe<sub>3</sub>O<sub>4</sub> [47], Li<sub>4</sub>Ti<sub>5</sub>O<sub>12</sub> [48], semi-crystalline Nb<sub>2</sub>O<sub>5</sub> [49], VO<sub>2</sub> [50], and layered titanates [51]. Nano-sized SnO<sub>2</sub> materials have been made previously via a continuous hydrothermal route, but have not been evaluated for lithium ion battery applications to date [52–54].

The as-prepared nano-sized doped materials were investigated using a range of analytical methods as well as being tested electrochemically as potential negative electrodes for lithium ion batteries. The transition metal dopants were grouped into two classes, namely (i) redox inactive and (ii) possible redox active dopants. Redox inactive dopants included Nb, Ti and Zr. Redox

active dopants included Fe, Co, Cu, Zn, Mn and Ni, which were classified because of the known ability of their corresponding metal oxides to undergo conversion (alloying) reactions with lithium ions [55,56]. The electrochemical performance of the as-prepared nanomaterials, was evaluated *via* potentiodynamic methods in order to assess the potentials versus lithium metal.

## 2. Experimental

### 2.1. Materials

All chemicals were used without further purification. Potassium stannate trihydrate (99.9%), titanium oxysulfate (≥29% Ti as TiO<sub>2</sub>), ammonium niobate oxalate hydrate (99.99%) and zinc nitrate hexahydrate (98%) were purchased from Sigma-Aldrich (Dorset, UK). Cobalt nitrate hexahydrate (99%), iron (III) citrate nonahydrate (98%), copper nitrate trihydrate (99%) and zirconyl nitrate hydrate (99.5%) were purchased from Fisher Scientific, (Leicestershire, UK). Manganese nitrate tetrahydrate (98%) and nickel nitrate hexahydrate (98%) were purchased from Alfa Aesar (Lancashire, UK). For the synthesis, 0.1 M of Sn salt was used for the production of undoped SnO<sub>2</sub> and 0.09 M of Sn salt mixed together with 0.01 M of the respective transition metal ion salt in solution, was used for the production of doped SnO<sub>2</sub>.

### 2.2. Synthesis

The nanoparticles were synthesized using a laboratory scale CHFS reactor incorporating a patented confined jet mixer (CJM), the basic design of which, can be found in the literature [57,58], see also supplementary Fig. S1. The CJM is essentially an efficient co-current mixing device made from off-the-shelf Swagelok<sup>TM</sup> fittings that efficiently allows the ambient temperature metal salt solutions to mix with the supercritical water feed to form nanoparticles “in flow” and without blockages. In the lab-scale CHFS process used herein [44], three identical diaphragm pumps (Primeroyal K, Milton Roy, Pont-Saint-Pierre, France) were used to supply three pressurized (24.1 MPa) feeds. Pump 1 supplied a feed of DI water at a flow rate of 80 mL min<sup>-1</sup>, which was then heated to 450 °C in flow using a 7 kW electrical water heater. Pump 2 supplied the metal salt precursors at a flow rate of 40 mL min<sup>-1</sup> and pump 3 supplied DI water at a flow rate of 40 mL min<sup>-1</sup>. The feeds from pumps 2 and 3 were combined at room temperature in a dead volume tee-piece before this mixture was then brought into contact with the flow of supercritical water (co-currently) in the CJM to give a calculated mixing temperature of ca. 335 °C (residence time ca. 5 s). Upon mixing of the hot and ambient temperature feeds in flow, the metal salts rapidly reacted to give the corresponding metal oxide nanoparticles that were then cooled to ca. 40 °C in flow over several minutes via a heat exchanger. At the end of the CHFS process, each of the cooled particle-laden aqueous flows passed through a back-pressure regulator (BPR) and was collected in a beaker. The resulting slurry was cleaned by allowing it to settle, before dialyzing the solids with DI water (<10 MΩ) and then freeze-drying (Virtis Genesis 35XL) by cooling to -60 °C followed by slow heating under a vacuum of < 13.3 Pa over 24 h. The freeze-dried powders were used for further analyses.

### 2.3. Materials Characterization

Powder X-ray diffraction (PXRD) patterns of all samples were obtained on a STOE diffractometer using Mo-Kα radiation (λ = 0.70926 Å) over the 2θ range 2 to 40° with a step size of 0.5° and step time of 20 s. X-ray photoelectron spectroscopy (XPS) measurements were collected using a Thermo Scientific K-alpha

Download English Version:

<https://daneshyari.com/en/article/6471232>

Download Persian Version:

<https://daneshyari.com/article/6471232>

[Daneshyari.com](https://daneshyari.com)